

The CML Air Bearing Dynamic Simulator

Yong Hu and David. B. Bogy
Computer Mechanics Laboratory
Department of Mechanical Engineering
University of California
Berkeley, CA94720

Abstract

This report presents a detailed description of the air bearing slider dynamic simulator developed at the Computer Mechanics Laboratory at the University of California at Berkeley. The code provides the numerical analysis of head-suspension assembly dynamics for shaped-rail sliders. The program simultaneously solves the generalized Reynolds equation and the equations of motion of the head-suspension assembly. The time-dependent nonlinear generalized Reynolds equation is directly discretized using Patankar's control volume method, in which the unsteady term is discretized in the implicit form. The final discretization equations are solved using the alternating direction line sweep method combined with a multi-grid method. The implementation of the multi-grid method dramatically improves the efficiency of the simulator. The slider's equations of motion are solved by a Newmark- β integration method to achieve high accuracy and less frequency distortion as compared to other commonly used methods. The program offers several specific applications for studying the dynamic effects on slider's flying performance. All of these features are described in detail and sample calculations are performed and presented along with graphical results for representative cases.

1 Introduction

This report is a manual for the air bearing dynamic simulator developed at the Computer Mechanics Laboratory at the University of California at Berkeley.

The code described in this report provides the numerical analysis of head-suspension assembly dynamics for shaped-rail sliders. The program simultaneously solves the generalized Reynolds equation and the equations of motion of the head-suspension assembly. The slider's motion is determined by the balance of the air bearing pressure, the suspension force, the contact forces and the inertia. The suspension force can be represented using either the flexure stiffness and damping coefficients or the suspension dynamics. As an alternative to the finite element solution for the suspension, a modal truncation method is used to include the contribution of the suspension assembly dynamics in the dynamic analysis. The suspension assembly equations of motion are transformed into modal coordinates. The method is very effective in reducing the dimensions of the numerical scheme for solving the equations of motion while retaining essential dynamic characteristics of the problem.

The time-dependent nonlinear generalized Reynolds equation is directly discretized using Patankar's control volume method. The final discretization equations are solved using the alternating direction line sweep method combined with a multi-grid method. Compared with conventional single-grid methods, the multi-grid methods solve the equations on a hierarchy of grids so that all frequency components of the error are reduced at comparable rates. Inexpensive iteration on the coarse grid rapidly diminishes exactly those components of the error that are so difficult and expensive to reduce by fine grid iteration alone. This results in a dramatic reduction of solution time, especially for the dynamic simulation, since it involves repeated solutions of the discretized Reynolds equation. An adaptive mesh method is also implemented in the program, which can adjust the grid distribution according to the pressure gradient. This usually results in a better usage of the available grid points. The slider's equations of motion are solved by a Newmark- β integration method to achieve high accuracy and less frequency distortion as compared to other commonly used methods. The numerical integration of the coupled equations

begins with the estimated displacements of the slider based on the velocities of the previous time step. Then the new displacements are calculated by considering the air bearing pressure and suspension forces at that configuration. These new displacements are compared with the results of the previous iteration step. The iteration ends when the maximum relative change of displacements is smaller than a certain number, which, then gives the final displacements of the slider at that time step.

The dynamic analysis starts with the initialization of the fly height, pitch, roll and the corresponding velocities. The simulator then solves the slider's response to one or a combination of dynamic inputs. A number of dynamic effects on the slider's fly performance can be studied using the simulator. Among these are:

Disk Asperities: This type of analysis tracks the slider's response to the passage of asperities on the disk surface. Four types of asperities are available; the sinusoidal asperity, the ellipsoidal asperity, the cylindrical asperity and the rectangular asperity. Their lateral size, height and orientation are adjustable.

Initial Impulse: Initial impulses are realized numerically by applying initial velocities to the slider. The slider's initial impulse response can be used to characterize the air bearing damping.

Point by Point Disk Track Profile: To have the most realistic simulation of a slider flying over a rough disk surface, the simulator allows the direct input of point by point track profile data. At each time step, the film thickness distribution under the slider is obtained through interpolation of the track profile. With this new film thickness distribution, the coupled system of equations is solved. One application of this feature is a numerical estimation of the head-disk spacing modulation caused by the moving disk surface profile.

Integration of Suspension Dynamics: With the head-disk spacing in hard disk drives rapidly approaching sub-25nm levels, the suspension assembly dynamics may contribute significantly to the overall dynamics of the slider. To obtain an analysis of this contribution, modal analysis of the suspension is employed in the simulator to represent the suspension's

effect on the slider's dynamics. The dynamic response of the suspension assembly is represented by a linear truncated combination of mode shapes.

Numerical Generation of Waviness on Disk Surface: Four types of disk waviness can be numerically generated by the program. They are the sinusoidal wave, the ellipsoidal asperity wave, the cylindrical asperity wave, and the rectangular asperity wave. The waviness can be either one dimensional or two dimensional. They have adjustable wavelength, amplitude and orientation. The radial zone where each waviness exists can also be defined by the input.

Time-Dependent Disk Velocity: The program allows the disk velocity to be variable with time. This is usually used for landing/take-off simulations. The time-dependent velocity data consists of pairs of (time, velocity) points. A linear relationship between adjacent data points is assumed. For landing/take-off studies, the simulation can be performed to/from zero disk speed. However, in these cases, an asperity-based contact model should be invoked to ensure a meaningful result.

Asperity Contact: Two asperity-based contact models are implemented in the program: the GW model (Greenwood and Williamson 1966) and the elastic-plastic model (Chang, Etsion and Bogy 1987). Both are of probabilistic models. The rough surface is represented by a collection of asperities. The surface roughness is assumed to be random, isotropic and Gaussian. The contact stresses are assumed to depend upon the relative profile of the two surfaces in contact, i.e. upon the shape of the gap between them before loading. The system may then be replaced by a flat, rigid surface in contact with a body having an composite modulus and a profile which results in the same undeformed gap between the surfaces. For the GW model, it is assumed that the contacting asperities deform elastically according to Hertz theory. The elastic-plastic model is similar to the GW model but requires volume conservation of a certain control volume of plastically deformed asperities. The friction force is assumed to follow Coulomb's law; the product of the normal contact force and a friction coefficient. During the simulation, the program computes at each time step the expected values of the normal contact force, the contact

moments and the friction force based on the film thickness distribution. These forces and moments are then used to calculate the motion of the slider.

Track Seeking Motion: Track access is a process for the slider to move from one track to another. This process involves head motion as well as the dynamics of the suspension. The radial displacement of the slider changes its skew angle and the relative disk velocity, while the slider's accelerations introduce inertia forces. Both of these can adversely affect the spacing between the slider and disk. A time dependent head accessing acceleration profile is imposed and the head velocities are obtained by numerical integration. During the track access motion, the program calculates at each time step the updated radial location, skew angle and relative velocity of the disk surface at each grid point in the bearing. The inertia force acting on the suspension assembly may have significant influence on the spacing modulation for today's high performance disk drives. To effectively include this contribution, we perform the integration of the suspension assembly dynamics using modal analysis.

Zone Texture/Transition Zone Profile: So-called "zone texturing" is one of the approaches to reduce the stiction force during take-off and still allow the use of very smooth disk surfaces in the data region. In this approach, a small annular ring of texture with relatively large surface roughness is provided for the area where the slider starts and stops, while in the data zone, where the slider flies over the disk, the surface is made very smooth. There is a transition zone between the texture zone and the smooth data zone, which is produced during the manufacturing process. The radial zone surface profile is defined by three points in the radial direction. This feature can also be used to describe the radial disk edge profile.

Numerical Generation of Waviness/Asperities on the Slider: Similarly to the disk surface, waviness/asperities can also be numerically generated for the slider surface.

Disk Flutter: The disk flutter simulation provides information on how the slider responds to disk vibrations. Here a vertical sinusoidal flutter is used. The flutter frequency and amplitude can be adjusted.

2 Input and Output Data Files

2.1 Data Input Summaries('dynamics.def').

```
*****Problem Definition*****
xl          yl          xg          yg          zg          halt
2.05e-3    0.7805      0.5         0.0         0.105       0.0
f0          xf0          yf0          amz          aip          air
3.0e-3     0.5           0.0         6.0e-6      2.18e-10    1.36e-10
rpm         dt           tf           ra           rif          rof
5400.0     1.0e-6        0.001       23.0e-3     10.0e-3     30.0e-3
*****Suspension*****
iact        xact        dact        vact        ske
1           38.0e-3     0.0         0.0         -9.1
isusp       nmodes      ncg          alfa         beta
0           10          2149        60.0        1.0e-5
skz         skp         skr          scz          scp          scr
18.0       1.146e-2   1.432e-2   0.002       1.58e-6     1.4e-6
*****Initial Flying Condition*****
hm          hp          hr          vz          vp          vr
2.9e-7     165.0e-6   158.0e-9   0.0         0.0         0.0
*****Solution Control*****
iqpo        akmax       emax        idisc
5           1.0e-7     1.0e-4     1
*****Grid Control*****
iadpt       isymmetry   ioldgrid    nx          ny          nsx          nsy
1           0           0           98          98          1           1
xnt(i), i=2,nsx
0.0
nxt(i), i=2,nsx
0
dxr(i), i=1,nsx
1.0
ynt(i), i=2, nsy
0.0
nyt(i), i=2,nsy
0
dyr(i), i=1,nsy
1.0
difmax      decay       ipmax
40.0        40.0       0
*****Point by Point Disk Track Profile*****
ims         nfx         dinit
0           1009       3.2
*****Numerical Generation of Disk Surface Topography*****
nwave       nzone       nasper
```

```

0          0          0
iwtype    wamp      wang  wthx  wthy  wpdx  wpyd  wrs  wre
zr1       zh1       zr2      zh2      zr3      zh3
iatype    aamp      aang      alocx      alocy      asizx      asizy
*****Numerical Generation of Slider Surface Topography*****
nswave    nsasper
0          0
iswtype   swamp     swang     swthx     swthy     swpdx  swpdy
isatype   saamp     saang     salocx     salocy     sasizx  sasizy
*****Track Seeking Motion*****
nap
0
tac        aac
*****Time-Dependent Disk Velocity Profile*****
nvp
0
tvp        vtd
*****Sinusoidal Disk Flutter*****
iflut     tsft      teft      fqft      amft
0          0          0.003     100000.0  10.0e-9
*****Asperity Contact*****
icmod     ey        ydst      pratio    frcoe
2          9.7135e+10  1.0e+10   0.3       0.3
ncz
1
sikm      ceta      rasper    rcts      rcte
3.0e-9    2.0e+12  10.0e-9   10.0e-3   30.0e-3
*****End of Input Data*****

```

2.2 Input File ‘dynamics.def’. The file ‘dynamics.def’ contains the parameters which define the slider geometry, the fly conditions and the dynamic inputs.

2.2.1 Problem definition

- xl : slider length [m].
- yl : slider width normalized with xl.
- xg : slider gravity x-position, normalized with xl, starting from leading edge.
- yg : slider gravity y-position, normalized with xl, starting from center towards outer edge.

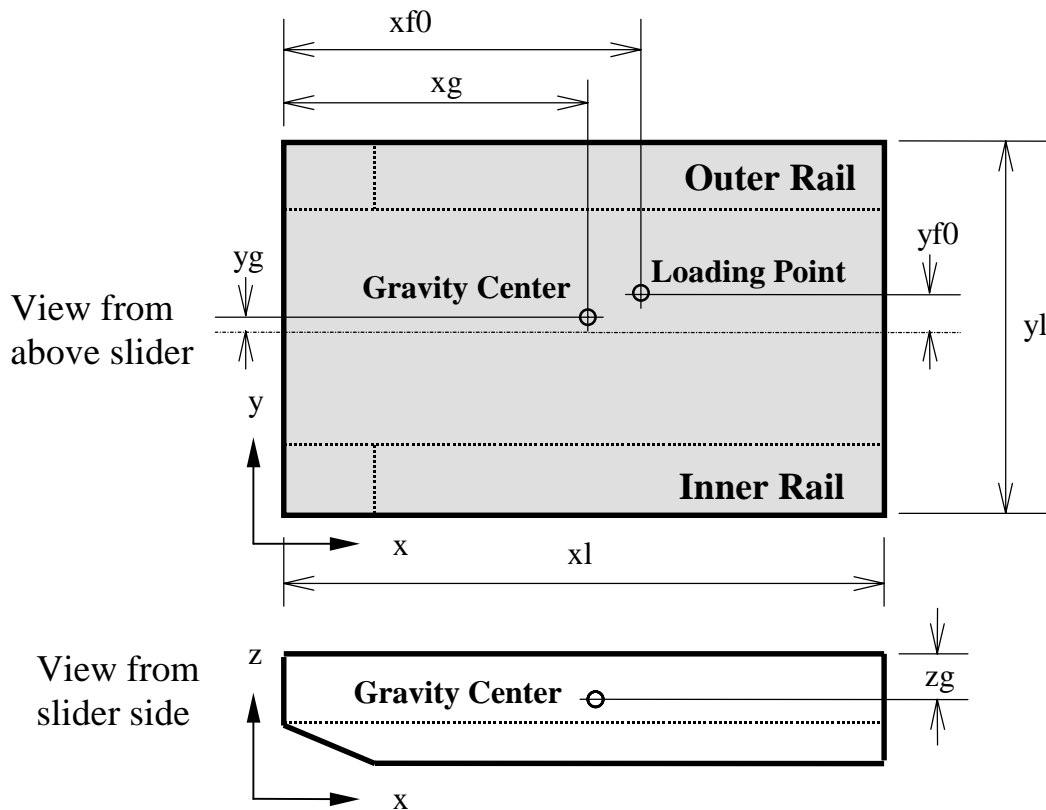
z_g : distance from the top of the slider to slider's gravity center in z direction, normalized with x_l .

$halt$: altitude above sea level [m].

f_0 : suspension load [kg].

xf_0 : load x-position, normalized with x_l , starting from leading edge.

yf_0 : load y-position, normalized with x_l , starting from center towards outer edge.



amz : slider mass [kg].

aip, air : slider pitch and roll moments of inertia, respectively [$kg \times m^2$].

rpm : disk revolutions per minute. It is initial rpm if the disk speed is time-dependent ($nvp > 0$).

dt, tf : time step and total time duration of the simulation, respectively [s].

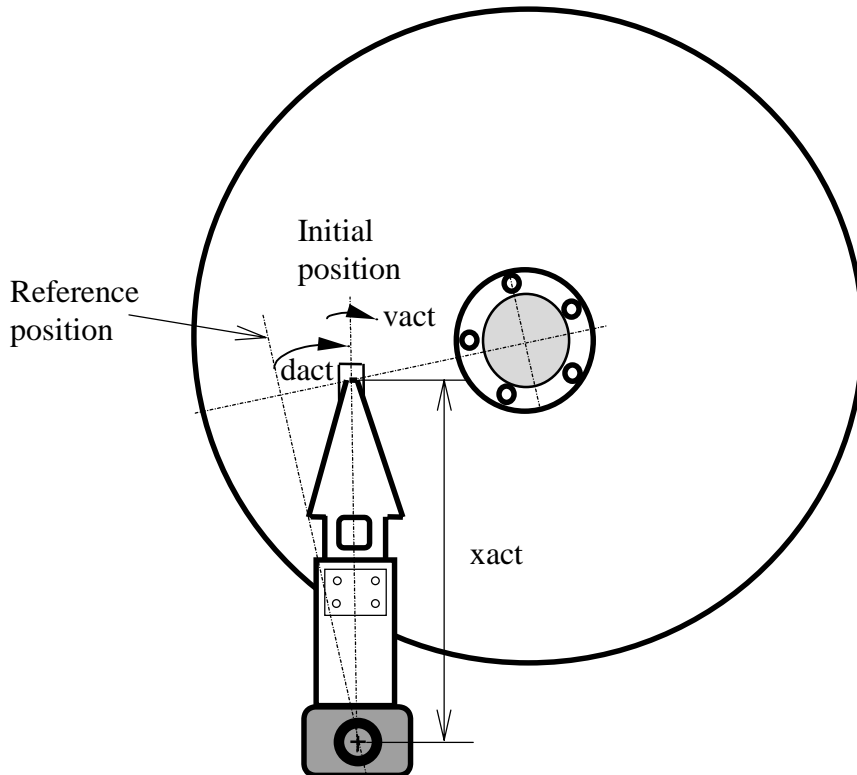
ra : radial position of the slider's gravity center [m]. It is initial radial position for the case of the off-track motion.

r_{if} , r_{of} : flyable inner and outer radial positions of the slider's gravity center, respectively [m].

2.2.2 Suspension

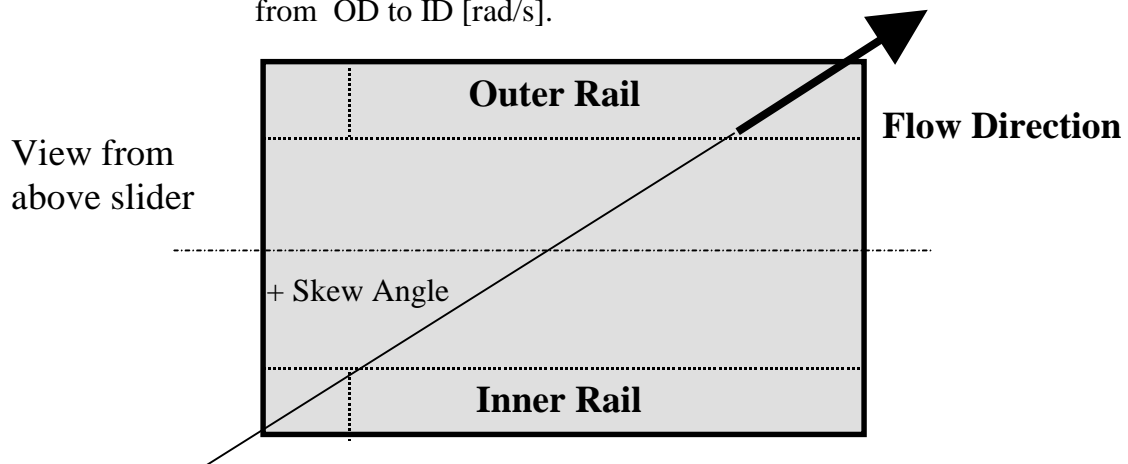
i_{act} : 0 = no actuator; 1 = inline actuator.

x_{act} : length of actuator arm [m].



d_{act} : angular position of actuator with respect to the reference position [rad].

v_{act} : angular velocity of actuator, positive velocity indicates that slider moves from OD to ID [rad/s].



skew	: initial skew angle [deg], positive skew implies that the air flows from the inner rail to the outer rail.
isusp	: 0 = using suspension stiffness and damping coefficients; 1 = integrating the suspension dynamics by modal analysis. When isusp = 1, two files 'fmodes.ext' and 'fmesh.inp' are needed. The file 'fmodes.ext' contains the natural frequencies and modal shapes. The file 'fmesh.inp' is the ABAQUS input file.
nmodes	: number of truncated suspension mode shapes. Used if isusp = 1.
ncg	: node number for the slider's gravity center defined in the ABAQUS input file. Used if isusp = 1.
alfa	: mass proportional suspension damping [s^{-1}]. Used if isusp = 1.
beta	: stiffness proportional suspension damping [s]. Used if isusp = 1.
skz	: vertical suspension stiffness coefficient [N/m]. Used if isusp = 0.
skp, skr	: pitch and roll suspension stiffness coefficients, respectively [$N \times m / rad$]. Used if isusp = 0.
scz	: vertical suspension damping coefficient [$N \times s / m$]. Used if isusp = 0.
scp, scr	: pitch and roll suspension damping coefficients, respectively [$N \times m \times s / rad$]. Used if isusp = 0.

2.2.3 Initial flying condition

hm	: initial nominal trailing edge center fly height [m]. Note that the reference point is on the nominal plane with pitch and roll, not including crown, camber or twist.
hp, hr	: initial pitch and roll, respectively [rad], positive roll indicates that the outer rail flies higher than the inner rail.
vz	: initial vertical impulse velocity at the slider gravity center [m/s].
vp, vr	: initial pitch and roll impulse velocities, respectively [rad/s].

2.2.4 Solution control

- iqpo : slip flow models, 0 = continuum; 1 = first order slip model; 2 = second order slip model; 5 = Fukui-Kaneko linearized Boltzman equation model. 5 is the recommended choice.
- akmax : normalized residual of Reynolds equation, criterion of convergence of the solver.
- emax : normalized difference between the predicted and the final values of flying heights at each time step, the criterion of convergence for the solution of slider motion.
- idisc : different schemes for treating the convective term. 1 = power-law; 2 = central difference; 3 = upwind; 4 = hybrid. idisc = 1 is recommended.

2.2.5 Grid control

- iadpt : 0 = disable adaptive grid; 1 = use adaptive grid.
- isymmetry : 0 = manually generate the grid over the whole slider width; 1 = generate only half of the grid, which is symmetrical in the slider width direction. This has no effect when the adaptive grid option is used.
- ioldgrid : 0 = either use adaptive grid or manually generated grid; 1 = use the old grid locations in the files 'x.dat' and 'y.dat'.
- nx, ny : grid size in x and y directions, respectively, must be in the form of $(16n+2)$ because of multi grid method. In the case of using old grid locations, nx and ny can also be in the form of $(16n+1)$ for consistency with the CML Air Bearing Design Program. Maximum nx and ny is 301.
- nsx, nsy : number of grid sections in x and y directions, respectively, for manually generated grids.
- xnt(i) : i from 2 to nsx, coordinates for the end of each section in the x direction, normalized with xl.
- nxt(i) : i from 2 to nsx, grid indices for the end of each section in the x direction.

dxr(i)	: i from 1 to nsx, ratio of grid size over previous one for each section in the x direction.
ynt(i)	: i from 2 to nsy, coordinates for the end of each section in the y direction, normalized with xl.
nyt(i)	: i from 2 to nsy, grid indices for the end of each section in the y direction.
dyr(i)	: i from 1 to nsy, ratio of grid size over previous one for each section in the y direction.
difmax	: used in the adaptive grid, a larger number allows a larger grid density difference.
decay	: used in the adaptive grid, a larger number has less smoothing effect, and the grid density depends more on the local pressure gradient and may change more abruptly.
ipmax	: used in the adaptive grid, 0 = use averaged pressure gradient in each direction along the cross section grid locations; 1 = use the maximum gradient in each direction along the cross section grid locations.

2.2.6 Point by point disk track profile

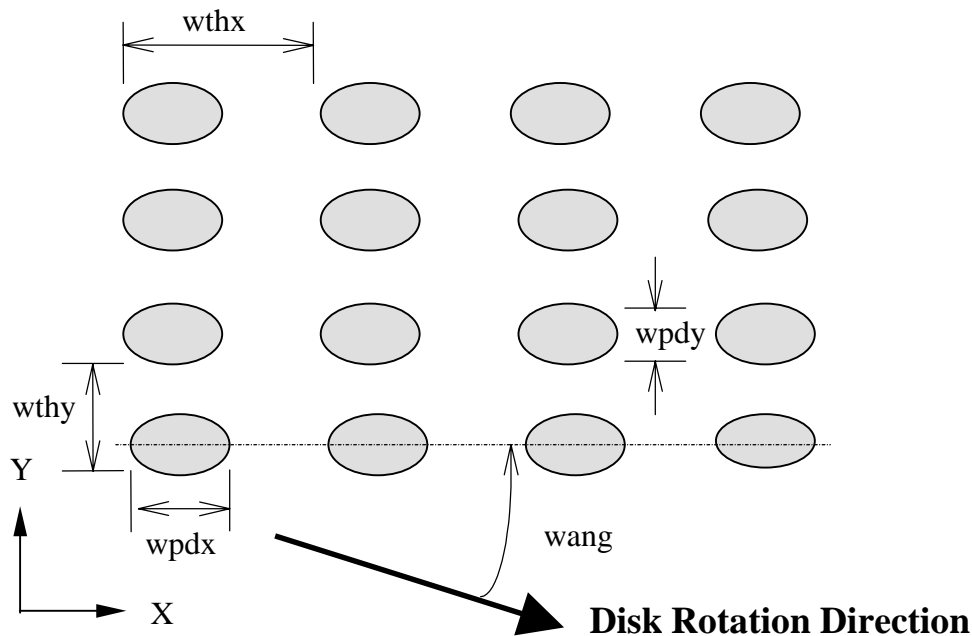
ims	: 0 = disable the point by point track profile; 1 = directly input the point by point track profile in the file 'wave.def'.
nfx	: number of track profile points. Maximum nfx is 1200. Used if ims = 1.
dinit	: initial location of the slider's gravity center from the first track profile location, normalized with xl. Used if ims = 1.

2.2.7 Numerical generation of disk surface topography

nwave	: total number of waves. Correspondingly, there should be the same number of lines to define these waves following the 'iwtype' line. Maximum nwave is 40.
nzone	: number of the radial zone profiles. Correspondingly, there should be the same number of lines to define the zone profiles following the 'zr1' line.

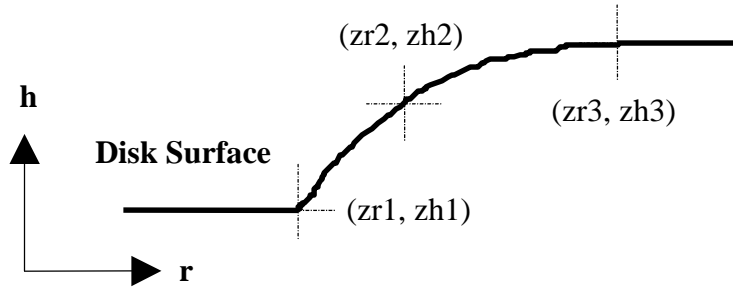
Each zone profile is defined by three radial points. The program can input up to 40 radial zone profiles.

- nasper** : number of asperities. Correspondingly, there should be the same number of lines to define the asperities following the 'iatype' line. Up to 40 asperities can be distributed over the disk surface.
- iwtype** : waviness type. 0 = sinusoidal wave; 1 = ellipsoidal asperity wave; 2 = cylindrical wave; 3 = rectangular asperity wave.
- wamp** : waviness amplitude [m].
- wang** : waviness orientation angle with respect to the disk rotation direction [deg].
- wthx,wthy** : wavelengths or repetition distances for the asperities in X and Y directions, respectively [m]. If one of them is zero, it implies the infinite wavelength in that direction.
- wpdx,wpdy** : pulse widths in X and Y directions, respectively [m]. If one of them is zero, it means the infinite pulse width in that direction. Not used for sinusoidal waviness.

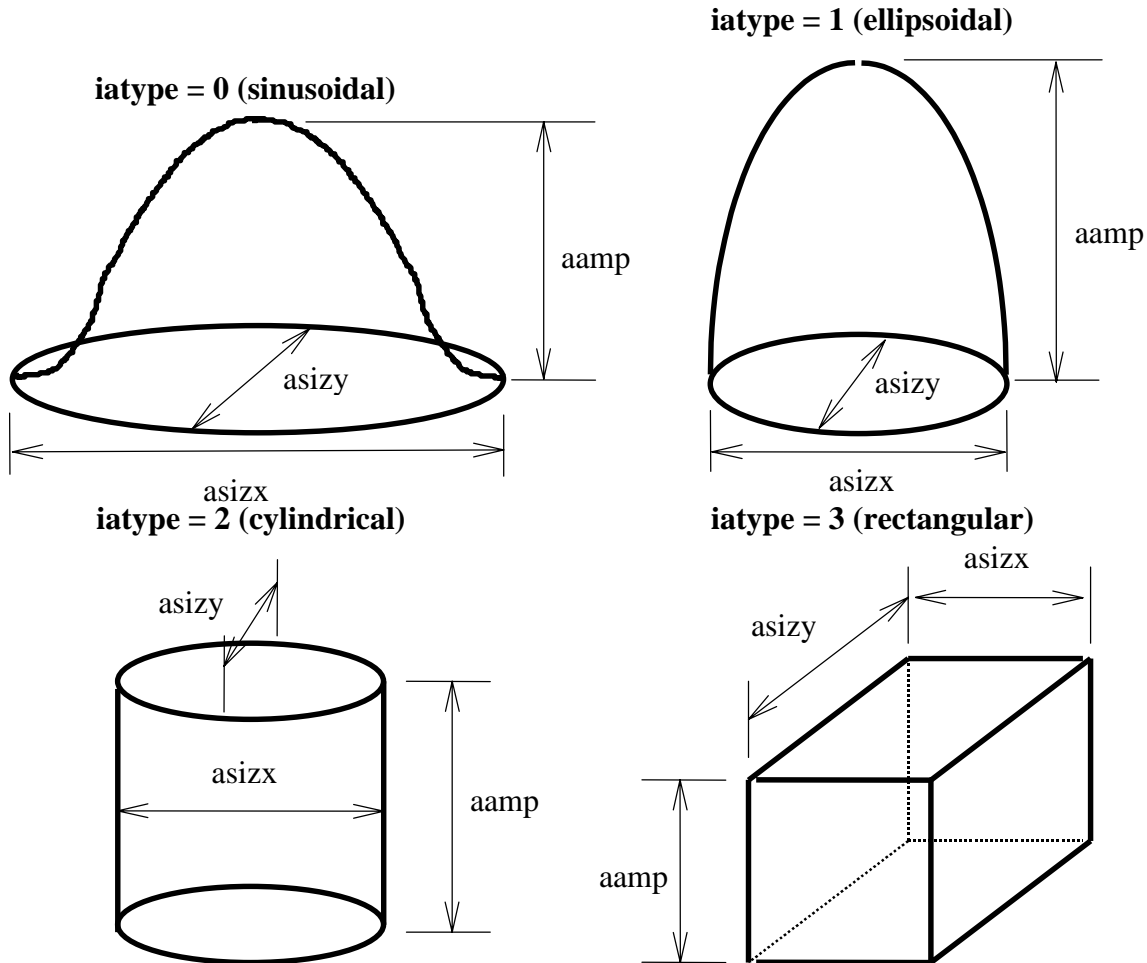


wrs, wre : starting and ending radii, respectively [m].

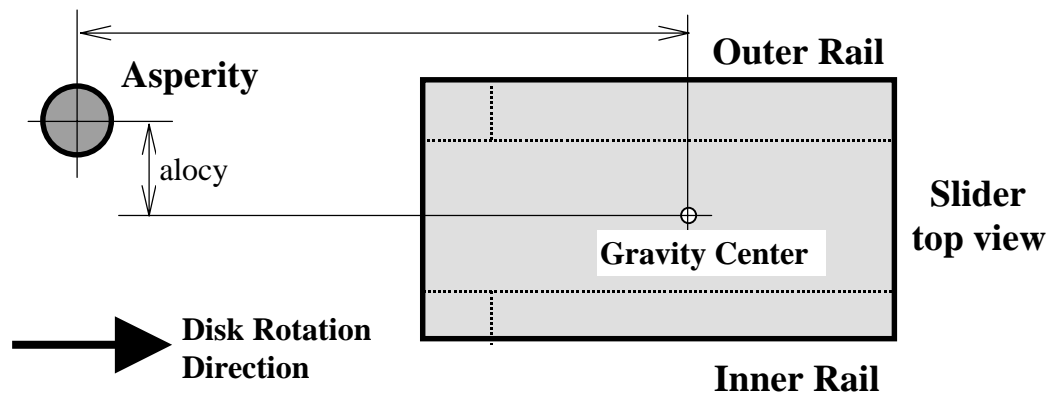
zrn, zhn : radius and height of point n ($n=1, 2, 3$), respectively [m]. Points 1 and 3 should be two boundary points. A parabolic functional relationship is assumed to exist for the three points.



iatype : asperity type. 0 = sinusoidal; 1 = ellipsoidal; 2 = cylindrical; 3 = rectangular.



- aamp** : asperity height [m].
- aang** : asperity orientation angle with respect to the disk rotation direction [deg].
- alocx,alocy** : asperity center location measured from the slider's gravity center at initial time in disk rotation and radial directions, respectively [m].
- asizx,asizy** : asperity footprint lengths in disk rotation and radial directions, respectively [m]. If one of them is zero, it implies the infinite size in that direction.



2.2.8 Numerical generation of slider surface topography

- nswave** : total number of waves on slider surface. Correspondingly, there should be the same number of lines to define these waves following the 'iswtype' line. Maximum nswave is 40.
- nsasper** : number of asperities on slider surface. Correspondingly, there should be the same number of lines to define the asperities following the 'isatype' line. The program can generate up to 40 asperities over the slider surface.
- iswtype** : waviness type. 0 = sinusoidal wave; 1 = ellipsoidal asperity wave; 2 = cylindrical wave; 3 = rectangular asperity wave.
- swamp** : waviness amplitude [m].
- swang** : waviness orientation angle with respect to x direction [deg].
- swthx,swthy** : wavelengths or repetition distances for the asperities in x and y directions, respectively [m]. If one of them is zero, it implies the infinite wavelength in that direction.

swpdx,swpdy : pulse widths in x and y directions, respectively [m]. Not used for sinusoidal waviness. If one of them is zero, it means the infinite pulse width in that direction.

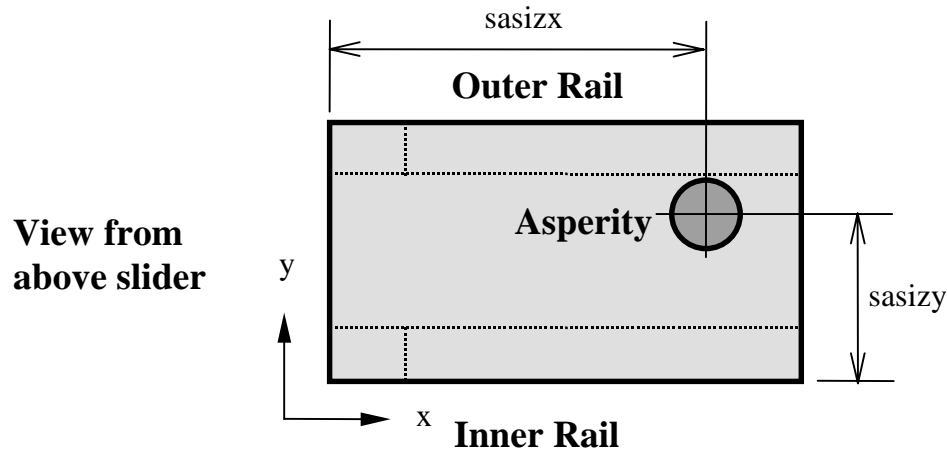
isatype : asperity type. 0 = sinusoidal; 1 = ellipsoidal; 2 = cylindrical; 3 = rectangular.

saamp : asperity height [m].

saang : asperity orientation angle with respect to x direction [deg].

salocx, salocy : asperity center location in x direction from the slider's leading edge and in y direction from the slider's inner rail boundary edge, respectively [m].

sasizx,sasizy : asperity footprint lengths in x and y directions, respectively [m]. If one of them is zero, it means the infinite size in that direction.



2.2.9 Track seeking motion

nap : number of points to follow which describe the acceleration/deceleration profile. A linear functional relationship is assumed to exist between adjacent data points. The program can input up to 40 data points.

tac : time [s].

aac : angular acceleration [rad/s²].

2.2.10 Time-dependent disk velocity profile

nvp : number of points used in describing the time-dependent disk velocity profile. Correspondingly, there should be the same number of data lines to define the speed profile following the ‘tvp’ line. The program can take up to 40 data points. If the simulation proceeds to times greater than that of data input, the value of velocity at the largest time will be used.

tvp : time [s].

vtd : disk rotational speed [rpm].

2.2.11 *Disk flutter*

iflut : 0 = disable disk flutter; 1 = disk flutter.

tsft, teft : starting and ending times of disk flutter [s].

fqft : flutter frequency [HZ].

amft : flutter amplitude [m].

2.2.12 *Asperity Contact*

icmod : 1 = GW model; 2 = elastic-plastic model.

ey : composite elastic modulus [Pa].

ydst : yield strength [Pa].

pratio : Poisson’s ratio.

frcoe : friction coefficient.

ncz : number of radial contact zones. There should be the same number of line data to follow which describe the roughness of each zone. Maximum ncz is 5.

sikm : composite standard deviation of the asperity heights [m].

ceta : area density of asperities [m²].

rasper : asperity radius of curvature [m].

rcts, rcte : starting and ending contact zone radii, respectively [m].

2.3 Input File ‘rail.dat’. The file ‘rail.dat’ defines the rail shape and air bearing surface. The rail shapes are defined by piece-wise linear boundaries. A rail can be a step with a given recess depth,

or it can be defined as a 'ramp', i.e., a flat plane having a specified orientation. Each rail may have a different recess depth. Normally, a zero recess is assigned to the main air bearing surface. The dynamic simulator shares the same 'rail.dat' file as the Air Bearing Design Program. For consistency, we directly copy the description of the file 'rail.dat' from the CML Air Bearing Design Program User's Manual (Sha and Bogy 1995).

The first line in 'rail.dat' indicates how many rails are defined and how many different recess heights they possess.

The data for each rail follow. First, the number of boundary points, the recess height index of the current rail and the number of points in the wall profile are given. The last number should be less than two if the rail is of the ramp type (the recess height index is 0). Next, the coordinates of the boundary points normalized with slider length are shown, with the origin at the inner leading edge. If the recess height index is 0, there is an additional line consisting of recess depths for the first three boundary points of the rail. Finally, if the wall profile has at least two points (otherwise a vertical wall is assumed), two more lines are used to describe it. The first line gives the coordinates of the points in terms of the normal distance to the nominal wall normalized by the slider length. Points with negative coordinates are inside the nominal rail boundary, and those with positive coordinates are outside the boundary. The second line contains the recess values (in meters) for the wall profile points.

After all the rails are defined, there is a line which gives the base recess depth (area not defined as rails), and rail recess depths in index order. All recess values are in meters. The next line shows taper length (normalized with slider length) and taper depth in meters. If a virtual taper exists, but is defined using 'ramps' instead of by the taper specification, the taper length should be set to the actual value, with zero taper depth at the front. The code will then try to resolve the taper end automatically when the adaptive grid is used.

The next line contains information on crown, twist and camber in meters. the crown is a longitudinal parabolic surface superimposed on the whole slider. A positive crown decreases the surface between the slider and the disk. The camber is the same as the crown except that it is in

the transverse direction. The twist is given in terms of the relative height of four corners to the center. A positive twist increases the separation between the slider and the disk at the inner leading edge and the outer trailing edge, and decreases the separation at the outer leading and inner trailing edge.

The last two lines give the x and y normalized coordinates of four points on the slider, respectively. The program outputs the fly height at these four points.

2.4 Other Input Files. The file ‘wave.def’ is needed for the simulation using the point by point disk track profile (ims = 1). The file contains two columns of data: position (meters) in column 1 and height (meters) in column 2. To integrate the suspension dynamics by modal analysis, you need to have two files ‘fmodes.ext’ and ‘fmesh.inp’. The file ‘fmodes.ext’ stores the natural frequencies and modal shapes. The file ‘fmesh.inp’ is the input file of the commercial FE code ABAQUS.

2.4 Output Files.

The output file ‘fhist.dat’ contains slider settling history. There are five columns of data: time (s) in column 1, nominal fly height (m) in column 2, pitch (rad) in column 3, roll (rad) in column 4 and off-track displacement (m) in column 5. The file ‘hpoint.dat’ stores the displacements (measured from the mean disk surface) at the four points defined in ‘rail.dat’. The corresponding disk floor heights at these four points are contained in the file ‘hfloor.dat’. The file ‘track.dat’ stores the following data: time (s) in column 1, radial position (m) in column 2, accessing velocity (m/s) in column 3, accessing acceleration (m/s^2) in column 4, geometrical skew angle (deg) in column 5, effective skew angle (deg) in column 6 and disk speed (rpm) in column 7. The effective skew angle is the angle between the slider’s length axis and the relative disk velocity vector.

Air bearing force history is stored in the file ‘load.dat’ which has four columns of data: time (s) in column 1, air bearing force (kg) in column 2, normalized air bearing force center XF in column 3, normalized air bearing force center YF in column 4, positive air bearing force (kg) in column 5, and negative air bearing force (kg) in column 6. The contact force history is saved

in the file 'contact.dat'. The file contains five columns of data: time(s) in column 1, the normal contact force (kg) in column 2, the contact moments in pitch direction (column 3) and roll direction (column 4) (N×m) as well as the ratio of the real to apparent contact area in column 5.

The files 'x.dat' and 'y.dat' contain the normalized x and y coordinates, respectively. The pressure matrix is stored in the file 'p2.dat'.

3 Examples of Dynamic Simulations

This section presents five sample simulations to demonstrate some of the features provided by the simulator. The Nutcracker slider designed in CML and built by Read-Rite was used for the sample calculations. It is a shaped-rail 50% sub-ambient pressure type slider. Figure 1 shows its air bearing surface. The slider has a 24 degrees wall angle from horizontal. The design target fly height is about 25nm under 3.5 grams of loading force. The slider design has a center rail that carries the read-write element. The read-write point is offset 25 μ m from the trailing edge. The slider has a 15nm crown. It is also designed with a positive 10nm camber so that the closest point is near the center rail trailing edge. The rail shapes are drawn in on both sides to minimize the fly height change across the disk. The connected front regions of the air bearing surfaces enable the efficient generation of the sub-ambient pressure in the central recessed regions. The disk rotational speed is 5400 rpm.

3.1 Bump and impulse responses. Figure 2 illustrates the slider's response to the passage of a 10nm high rectangular bump on the disk surface. The bump has a width of 25 μ m and length of 2mm. The bump is initially located 1.5mm ahead of the slider's gravity center. The slider reacts slightly as the bump travels under the front taper and then experiences larger oscillation as the bump encounters the more sensitive lower film thickness portions of the bearing. Figure 3 shows the slider's impulse response to the initial vertical velocity of 5.88mm/s.

3.2 Spacing modulation over a "supersmooth" disk. When the slider flies over a real disk, the inevitable surface roughness causes fluctuations in the head-disk spacing. In our simulation, a measured disk track profile is directly incorporated. Figure 4 shows a measured supersmooth disk

track profile with a long wavelength cut-off of 350 μm . The corresponding fly height, pitch, roll and air bearing force are also plotted in the same figure and their fly height and roll modulations are summarized in Table 1.

3.3 Track seeking dynamics. In this simulation, the suspension dynamics is integrated by modal analysis ($\text{isusp} = 1$). The FEM mesh of a Hutchinson 1650E type suspension is displayed in Fig. 5. 3331 nodes are used to model this suspension with a dense mesh distribution in the portion of the integrated gimbal. The eigenvalue solution is first sought using ABAQUS, then the first 10 modes are used in the air bearing simulation to represent the suspension dynamics during the track seeking event. Figure 6 presents the track accessing profile. To move the slider from 23mm to 13.78 mm in the radial direction, it is first accelerated to 1.91 m/s, followed by 0.9 ms of constant velocity, then decelerated to 0 velocity. The maximum acceleration/deceleration is 50g. During the whole process, the geometrical skew angle changes from -8.32 to 10.58 degrees. Figure 7 shows the slider's flying characteristics. The fly height modulation is closely related to the roll motion caused by the inertia force. The fly height modulation pattern shown depends on the read-write element location and the accessing direction. Since the read-write transducer for the Nutcracker slider is located at the center trailing edge, the roll motion always results in an increase of the fly height. The pitch and the fly height change do not appear to be related. The pitch is affected very little by the slider's inertia force of the off-track motion. Figure 7 also shows that a transient oscillation in roll and off-track displacement follows the sudden roll change due to the sudden action of the slider's inertia force.

3.4 Contact start and stop over “zone texture/transition zone”. Figure 8 shows a schematic of the CSS process, which can be divided into the following stages: contact/take-off over CSS track, glide radially outward over CSS zone (zone texture), climb up transition zone (zone texture), glide radially outward over data zone (smooth surface), glide radially inward over data zone, climb down transition zone, glide radially inward over CSS zone and land/contact over CSS track. The whole CSS process lasts for 20 ms. It is recognized that this is much too fast, but this rate was chosen to demonstrate the capability more than the result. Large computations are

required to complete the process at normal rates. The CSS profiles are shown in Fig. 9. The CSS track and final data track are located at radii of 15mm and 19.96mm, respectively. The transition zone is a constant slope plane with a height of 25 nm. It starts at the radius of 16.5 mm and ends at the radius of 17 mm. The CSS zone and transition zone have a radially oriented sinusoidal texture with an amplitude of 5nm and wavelength of 148.5 μm . In addition to the zone texture, they have 3 nm of standard deviation of surface roughness. The data zone has 1 nm of standard deviation of surface roughness. Figure 10 presents the flying characteristics of the whole CSS process. Figure 11 illustrates the flying characteristics during contact take-off. Initially, the slider is at rest on the disk surface. At 0.1 ms, the disk begins to rotate. Due to the positive crown and the contact friction force at the interface, the slider pitches forward, resulting in an initial increase of the trailing edge fly height. After the initial start-up, the trailing edge fly height decreases, reaching a minimum of 3.2 nm at about 395 rpm, and then increases with disk speed. The flying characteristics during gliding outward over CSS zone is shown in Fig. 12. The radial sinusoidal texture causes a fluctuation in the head-disk spacing. During the climbing up transition zone, the fly height changes from a maximum to a minimum as shown in Fig. 13. This is because the contact with the asperities on the two side walls increases the fly height at the center trailing edge when the slider glides over the bottom of the transition zone; the lack of the contact on the two side walls decreases the fly height at the center trailing edge when the slider glides over the top of transition zone. Figure 14 illustrates the flying characteristics during the contact landing. As the disk spins down, the trailing edge fly height descends below the at-rest spacing, and then ascends a little above the at-rest spacing due to the forward pitching caused by the friction at the interface. Interestingly, after the spindle stops rotation, the slider rocks mainly on its camber instead of crown for a short period before fully settling down to the equilibrium position. This is because of its smaller roll stiffness.

References

Chang, W. R., Etsion, I., and Bogy, D. B., 1987, "An Elastic-Plastic Model for the Contact of Rough Surfaces," *ASME Journal of Tribology*, Vol.109, pp.257-263.

Greenwood, J. A., and Williamson, J. B. P., 1966, "Contact of Nominally Flat Surface," *Proceedings Royal Society (London)*, Series A295, pp.300-319.

Lu, S., and Bogy, D. B., 1995, "CML Air Bearing Design Program User's Manual," *Technical Report No. 95-003*, Computer Mechanics Laboratory, U.C. Berkeley.

	Mean Value	Modulation
Fly Height (nm)	23.4844	+5.3042 (22.59%) -4.0908 (17.42%)
Roll (μ rad)	-0.5903	+6.7308 -5.9155

Table 1 Summary of fly height and roll modulations

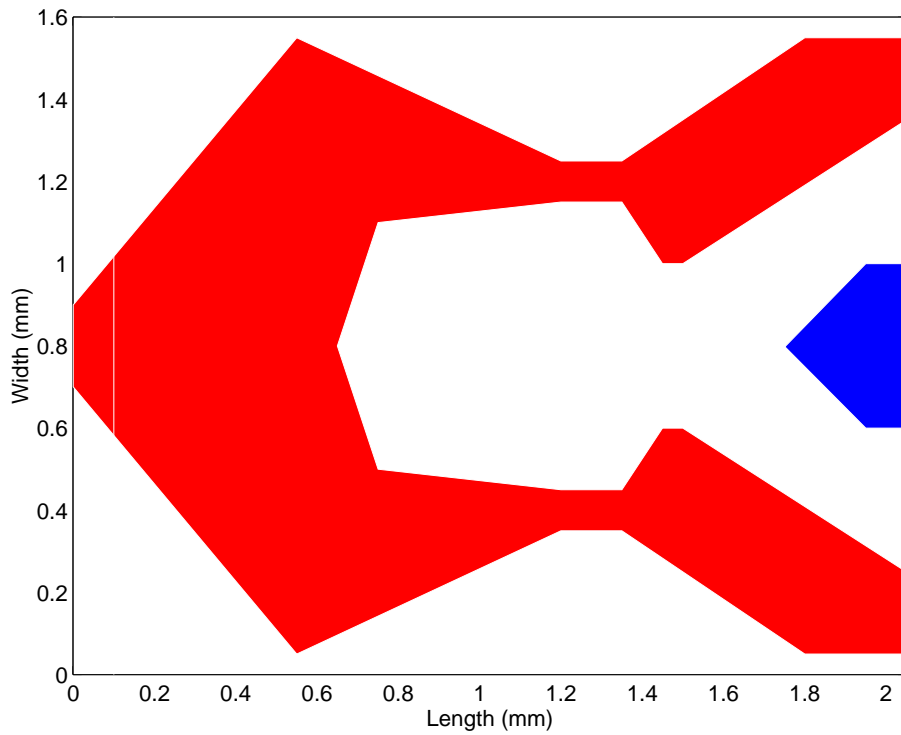


Figure 1 Air bearing surface for the Nutcracker slider

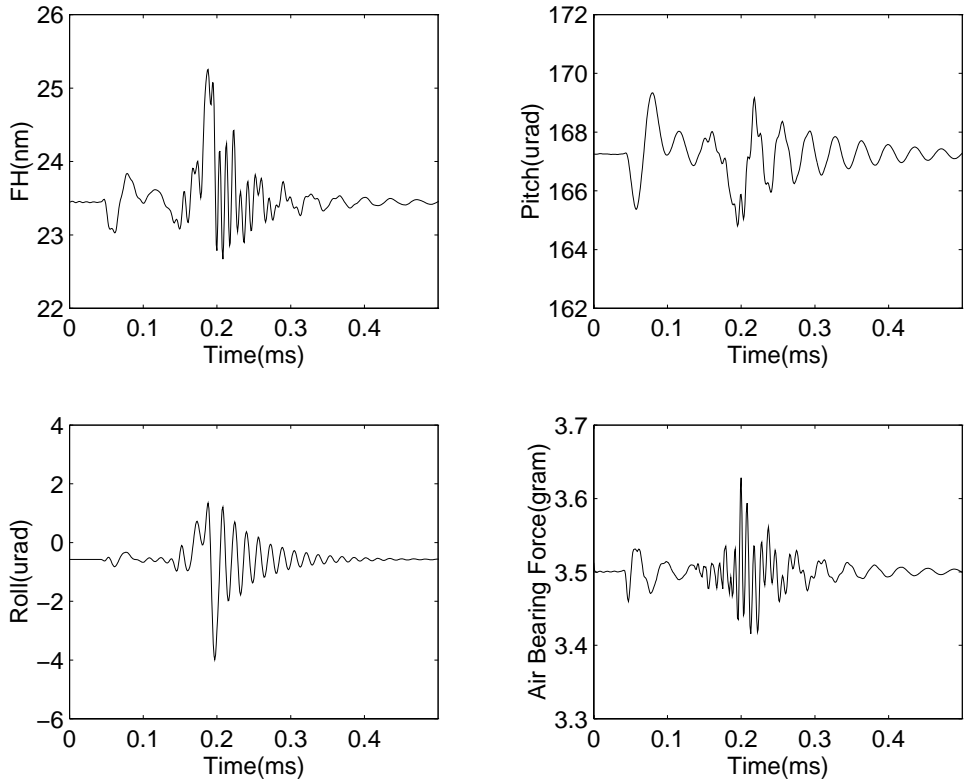


Figure 2 Bump response

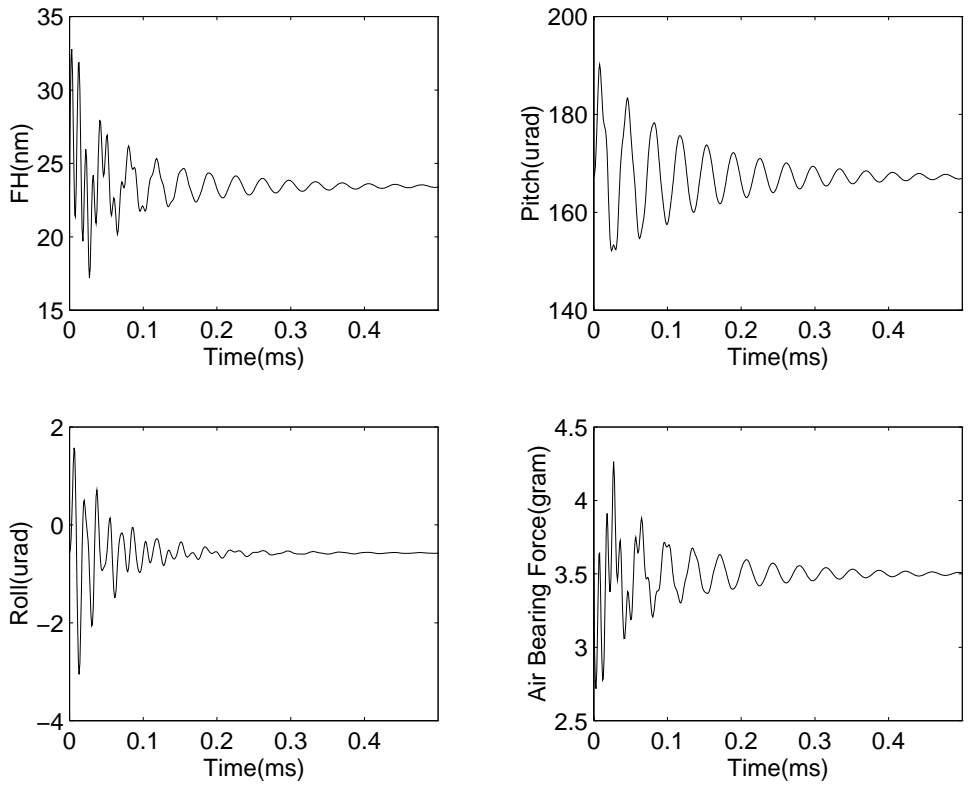


Figure 3 Impulse response

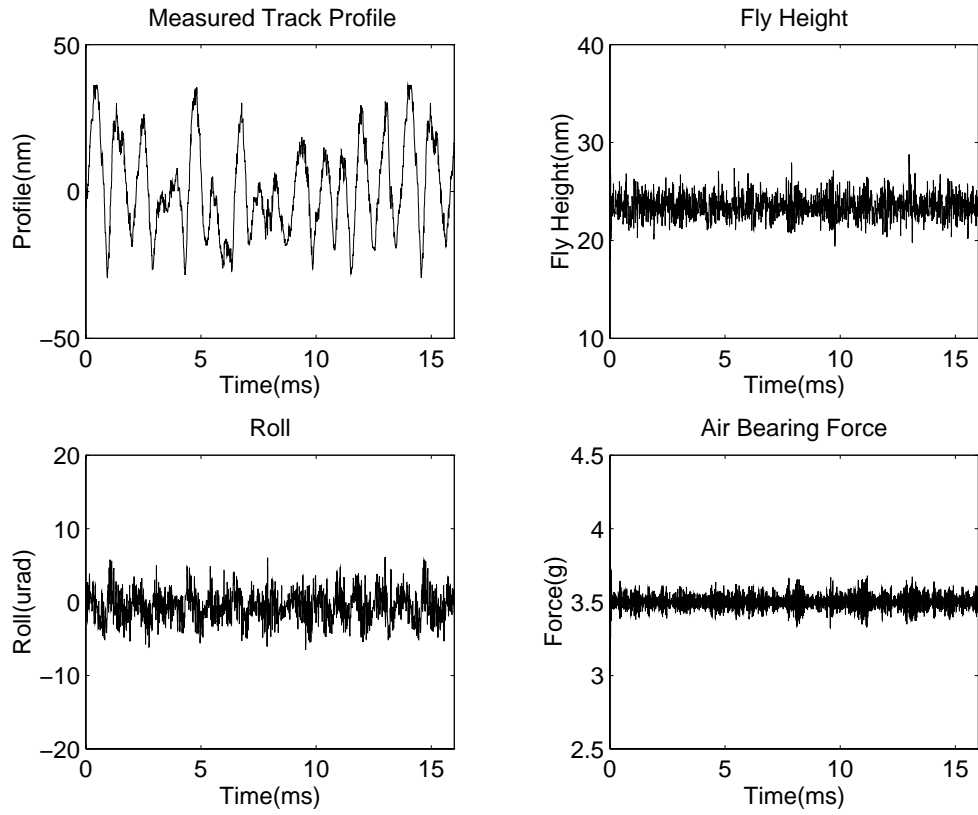


Figure 4 Fly height, pitch, roll and air bearing force modulations

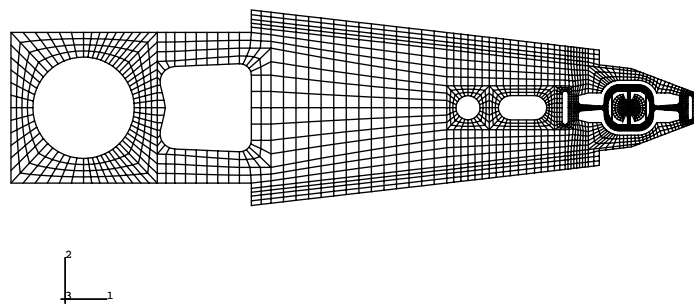


Figure 5 FEM mesh of a Hutchinson 1650E type suspension

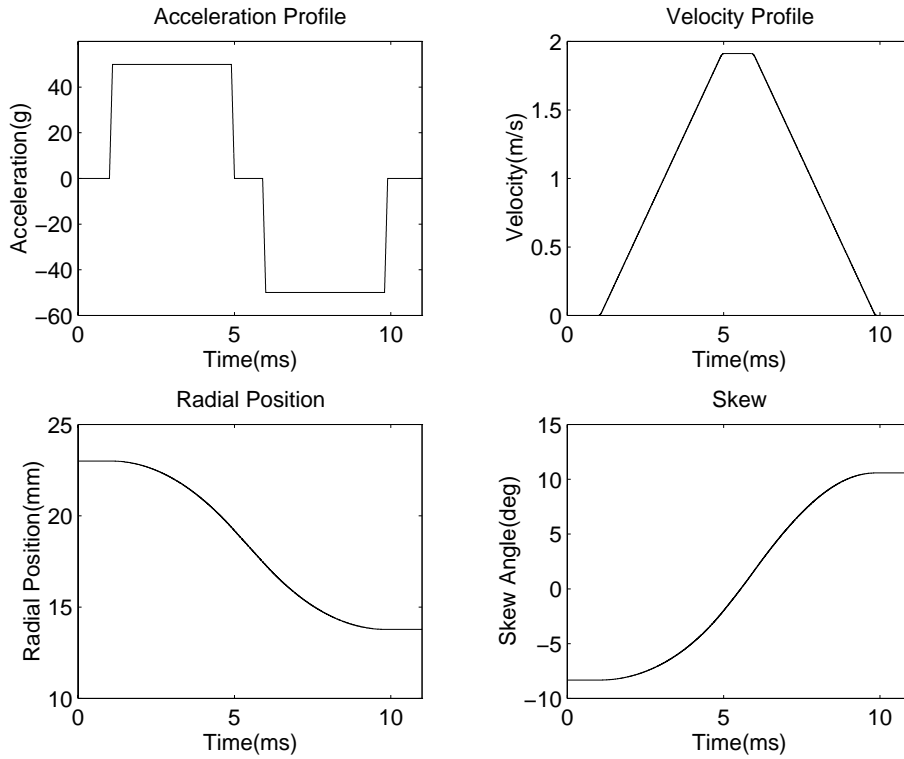


Figure 6 Track seeking profile

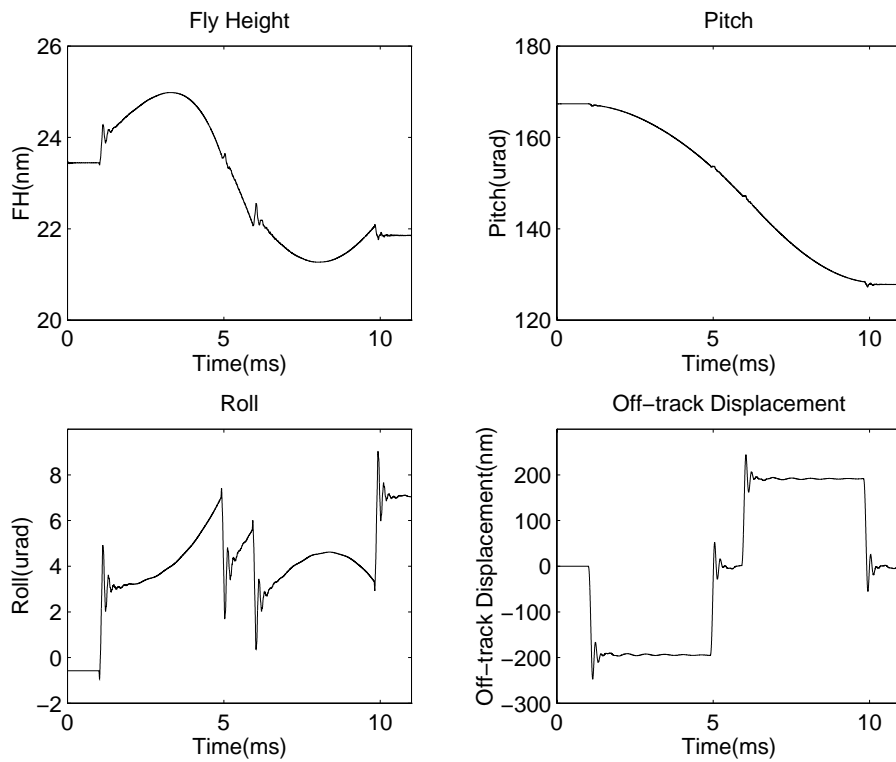


Figure 7 Fly characteristics during track access

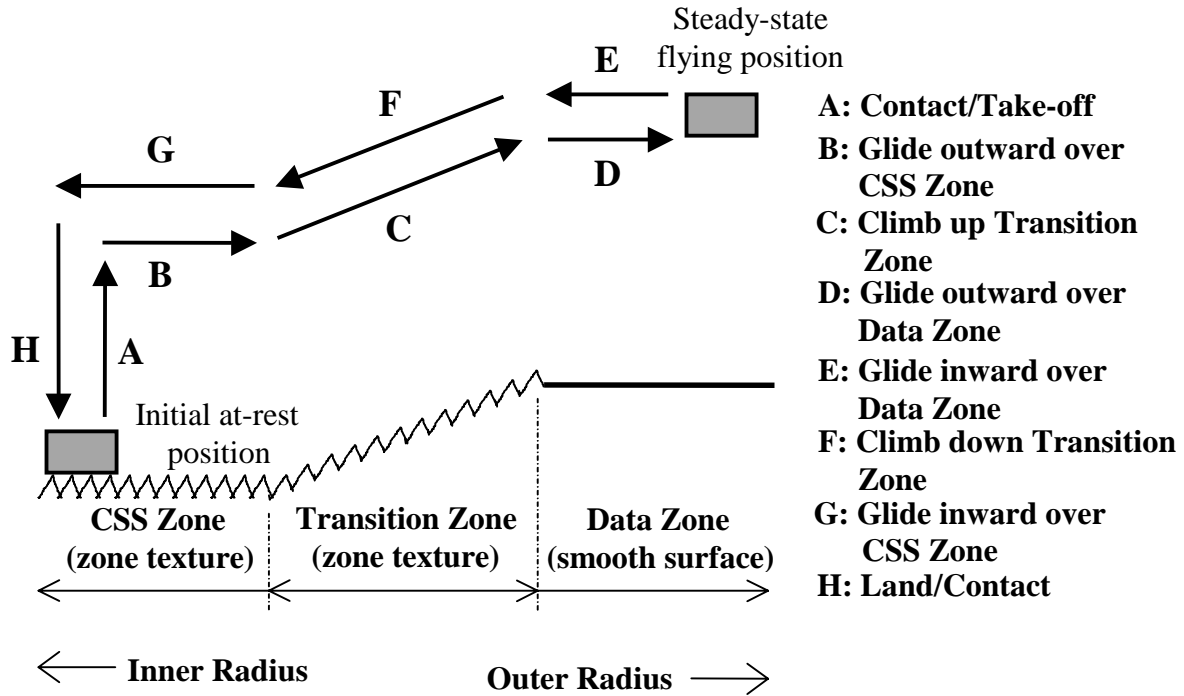


Figure 8 A schematic of the CSS over “zone texture/transition zone”

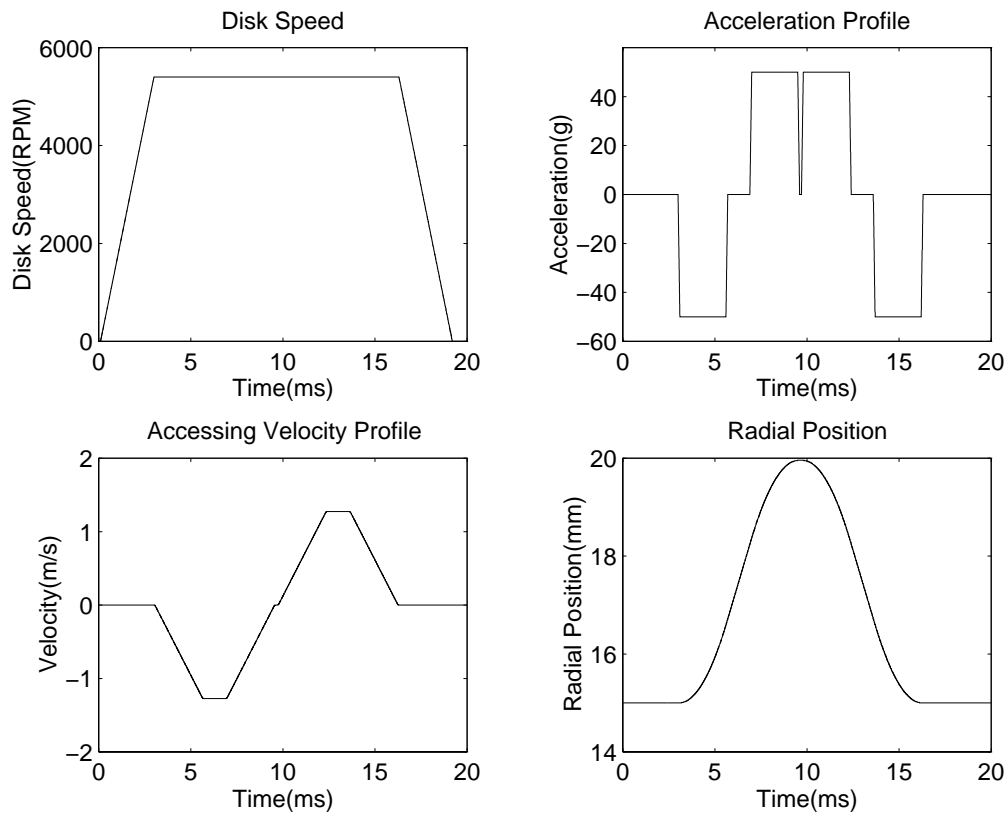


Figure 9 Profiles for the contact start and stop process

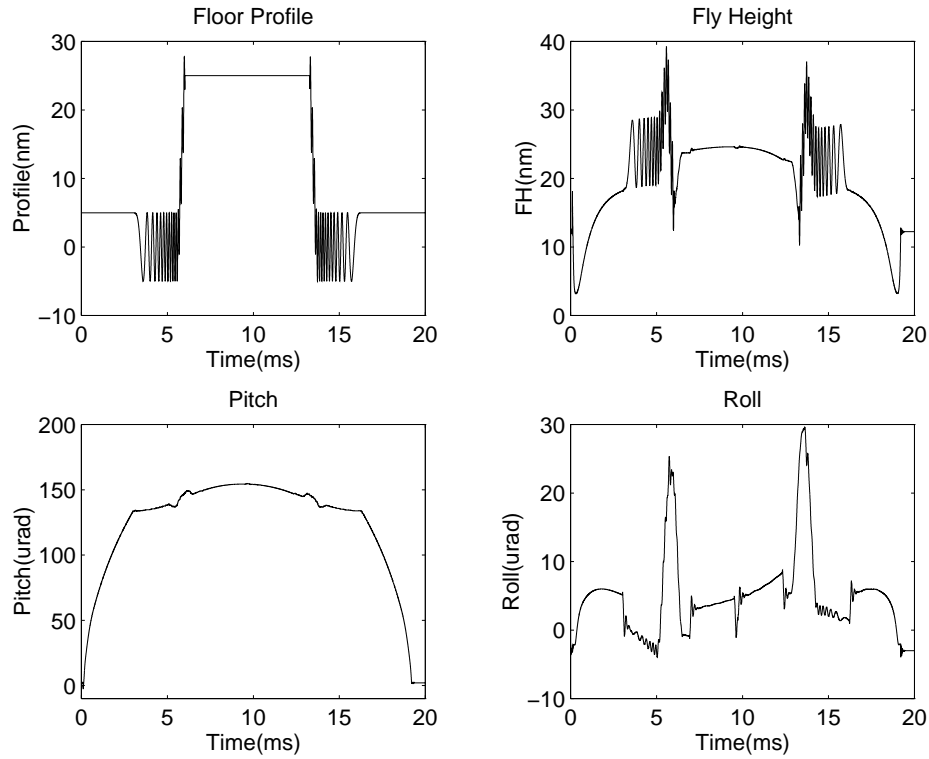


Figure 10 Flying characteristics of the CSS over “zone texture/transition zone”

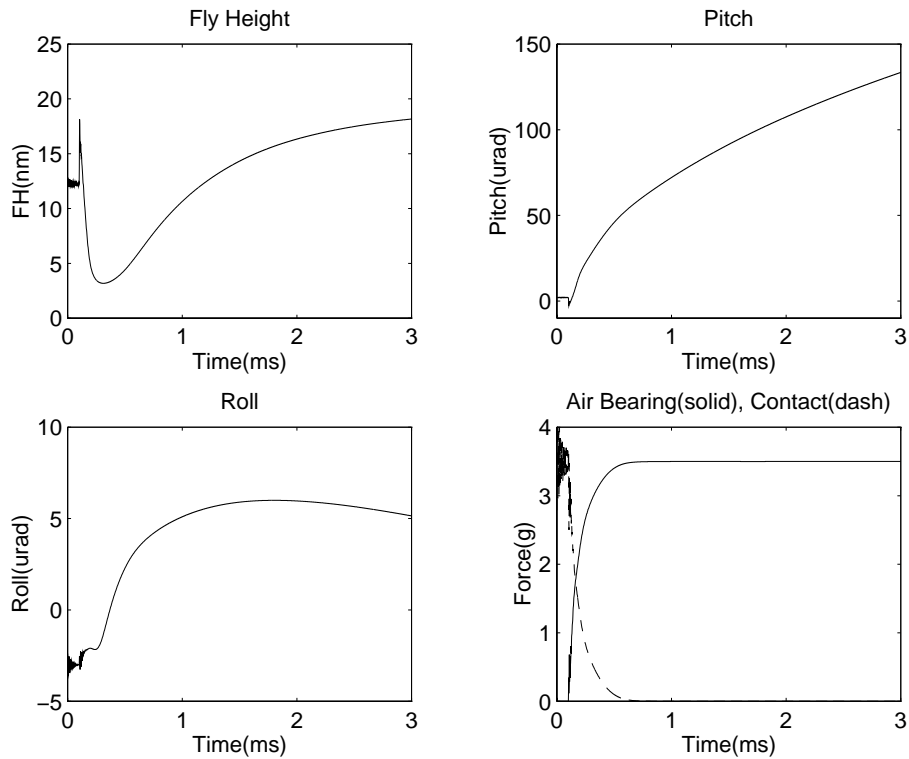


Figure 11 Flying characteristics of the contact take-off

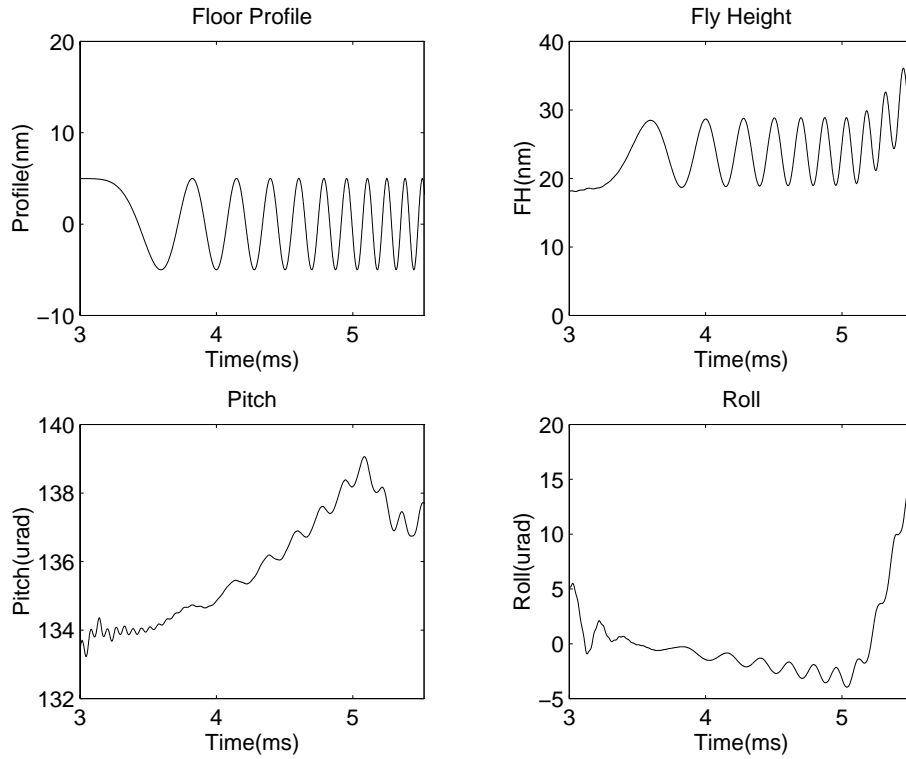


Figure 12 Flying characteristics during gliding radially outward over CSS zone

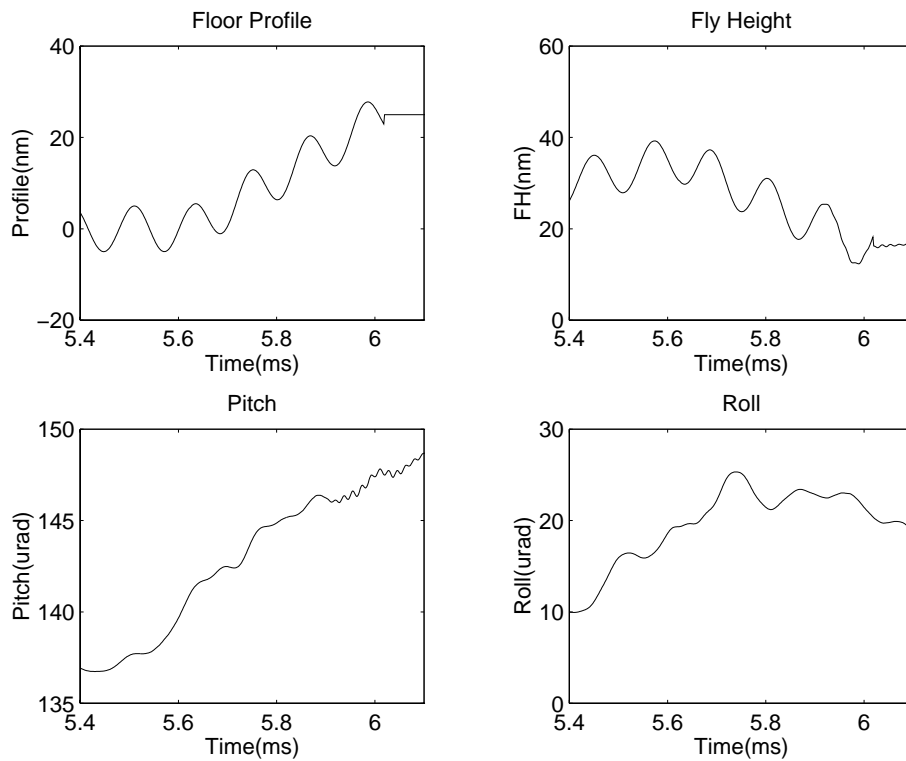


Figure 13 Flying characteristics during climbing up transition zone

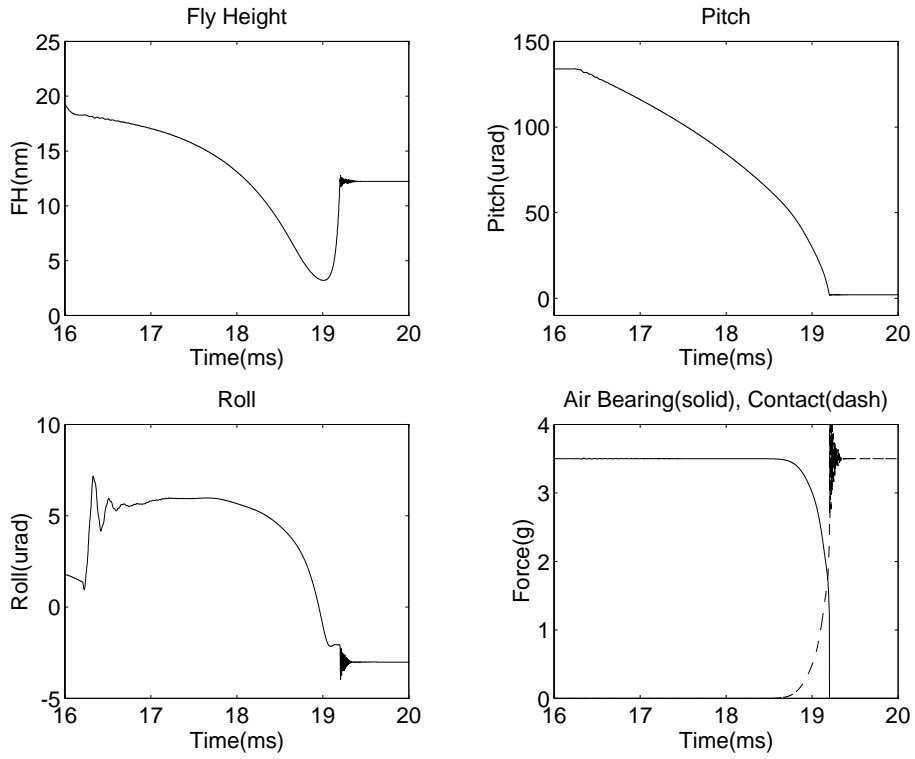


Figure 14 Flying characteristics during the contact landing